2D Green's theorem separation of reference wave and scattered wave in the (x-omega) domain using a depth-variable cable towards on-shore and ocean bottom application with variable topography

Zhen Zhang and Arthur B. Weglein, M-OSRP/Physics Dept./University of Houston*

SUMMARY

Green's theorem derived methods for separating the reference and scattered wavefields in the (x-ω) domain using flat cable have been successfully applied to synthetic and field data. Based on Green's theorem wavefield separation concepts, this paper derives a 2D acoustic P_0/P_s separation formula for a depth-variable cable assuming the shape of cable is known. In numerical tests, the air-water boundary is assumed to be horizontal. We use the Cagniard-de Hoop method to generate synthetic data on a parabolic cable and on a periodically semi-circular cable, respectively. The normal derivative of the total field on the cable is assumed to be known and is estimated by finite difference. Numerical results show that current Green's theorem P_0/P_s separation formula for a constant depth cable remains useful for a mildly depth-variable cable. When the actual cable deviates significantly from horizontal, the horizontal cable formula produces serious errors and artifacts whereas the new formula produces an effective and satisfactory result. While the analysis and tests in this paper are based on non-horizontal towed streamers, the motivation (and future work) is for on-shore and ocean bottom acquisition. Under these circumstances, the deviation from horizontal acquisition can be significant and the ability to accommodate a variable topography can have a considerably positive impact on subsequence processing and interpretation objectives.

INTRODUCTION

Green's theorem can offer a number of useful algorithms (Zhang (2007); Mayhan (2013)) that concern the broad field of seismic exploration (e.g. deghosting, P_0/P_s separation), by choosing reference medium for certain objectives. Figure 1 shows specific algorithms based on Green's theorem and inverse scattering series (Weglein et al. (2003)). As we can see, the first step is separation of reference wave (P_0) and scattered wave (P_s).

In marine prospecting, P_0 wave does not experience reflection from earth. Due to the presence of the air-water boundary, it includes two parts. One is called direct wave (G_0^d), which travels directly from the source to the receiver; the other is the ghost of the direct wave (G_0^{FS}) which travels up from the source to the air-water boundary and then gets reflected back to the receivers. Since P_0 wave travels only in water, it can be used to estimate source signature (Weglein and Secrest (1990)) without assumptions about the earth and water depth.

The P_s wave, which does experience the earth, can also be separated into two parts: those events moving upward to the receivers and those events moving downward to the receivers. And the upgoing part can be further separated into multiples and primaries, as shown by Figure 1. Weglein et al. (2003) described how every inverse scattering series (ISS) isolated-task

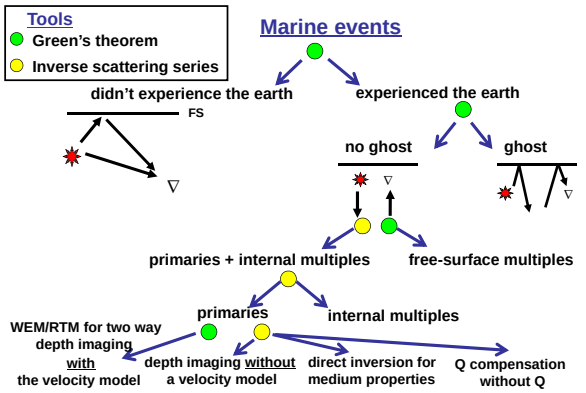

Figure 1: Application of Green's theorem and inverse scattering series (ISS) (Mayhan (2013)), by Mission-Oriented Seismic Research Program (M-OSRP) consortium.

subseries requires (1) the removal of the reference wavefield, (2) an estimate of the source signature and radiation pattern, and (3) source and receiver deghosting, and how the ISS has a nonlinear dependence on these preprocessing steps.

Green's theorem has proven to be a useful tool for wavefield separation. Weglein and Secrest (1988,1990) proposed a general wave theoretic P_0/P_s separation and wavelet estimation method through comparing the Lippmann-Schwinger equation and Green's theorem, given a cable (or in 3D, a surface) where both the pressure and its normal derivative are measured. Tests were done by Keho et al. (1990). To get rid of the need of normal derivative, Weglein et al. (2000) and Guo et al. (2005) developed P_0/P_s wave separation and source wavelet estimation algorithms that requires only the pressure on one cable, by means of Green's theorem wavefield prediction. Zhang (2007) summarized these wavefield separation and prediction algorithms and discussed their assumptions, limitations and advantages. The P_0/P_s separation methods mentioned above are in (x-ω) domain, where the P_0 or P_s wave is predicted either below or above the measurement surface. For on-shore exploration, Tang (2014) proposed the algorithm of P_0/P_s separation on exactly the cable in (k,ω) domain.

As pointed out by Mayhan and Weglein (2013) and Weglein et al. (2013), wavefield separation methods derived from the representation theorem are wave-theoretic algorithms that can be defined in the space-frequency domain and succeed in cables of any shape. The main objective of nonhorizontal measurement methods is to accommodate on-shore and ocean bottom acquisition where deviation from horizontal acquisition can frequently occur. Therefore, based on Weglein and Secrest (1990), we propose a 2D formula to separate P_s wave in the (x-ω) domain using depth-variable cables. Then P_0 wave is available through subtracting P_s wave from the total wavefield.

THEORY

Figure 2 shows the principle of 2D offshore Green's theorem P_0/P_s separation. It requires a one-shot record. The airgun is at $\mathbf{r}_s$. The receivers (green triangles) lie on a measurement line which can be nonflat. $\mathbf{r}$ is where we want to predict P_s wave using pressure measured by these receivers. According to Green's theorem wavefield separation theory, it can be anywhere above the measurement line and below the air-water boundary. Here we let $\mathbf{r}$ be below the source and not far away from the measurement line.

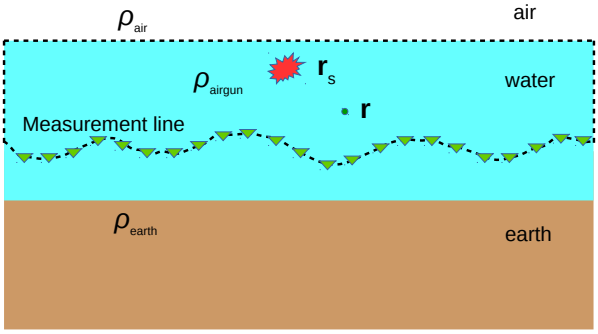

Figure 2: Configuration of Green's theorem P_0/P_s separation. The integration contour is the dashed line. ρ_{airgun} and ρ_{earth} overlay the reference medium (half space water and half space of air) to give the actual medium.

According to scattering theory, choose the reference medium to be half space of water (with acoustic speed c_0) and half space of air. Here the effect of air is assumed to be approximate to the effect of vacuum, so there is a free surface between air and water. Based on such reference medium, there are two sources in the actual medium: the airgun ρ_{airgun}, and medium perturbation ρ_{earth} due to the difference between earth and water. The reference field, which can be derived from the method of images (Morse and Feshbach (1953)), is $A(\omega)G_0(\mathbf{r},\mathbf{r}_s,\omega)$, where $G_0(\mathbf{r},\mathbf{r}_s,\omega)=G_0^d(\mathbf{r},\mathbf{r}_s,\omega)+G_0^{FS}(\mathbf{r},\mathbf{r}_s,\omega)$ and $A(\omega)$ is source wavelet. Here $G_0^d(\mathbf{r},\mathbf{r}_s,\omega)=-\frac{i}{4}H_0^{(1)}(kR_+)$ is the causal whole space Green's function, $H_0^{(1)}$ is the zeroth order Hankel function of the first kind, $k=\omega/c_0$, and $R_+=|\mathbf{r}-\mathbf{r}_s|$. $G_0^{FS}(\mathbf{r},\mathbf{r}_s,\omega)=\frac{i}{4}H_0^{(1)}(kR_-)$, $R_-=|\mathbf{r}-\mathbf{r}_{sI}|$ and $\mathbf{r}_{sI}$ is the mirror image of $\mathbf{r}_s$ with respect to the free surface. Based on Green's theorem, the P_s wave is (Weglein and Secrest (1990) and Mayhan (2013)),

$$P_s(\mathbf{r},\mathbf{r}_s,\omega)=\oint_l[P(\mathbf{r}',\mathbf{r}_s,\omega)\nabla' G_0(\mathbf{r}',\mathbf{r},\omega)-G_0(\mathbf{r}',\mathbf{r},\omega)\nabla' P(\mathbf{r}',\mathbf{r}_s,\omega)]\cdot d\mathbf{l}' \quad (1)$$

where P is input total field observed at $\mathbf{r}'=(x',z')$. $d\mathbf{l}'$ is the line element vector of the contour. Here we give the formula for 2D case, which can be proved using 2D Green's second identity. Since both P and G_0 vanishes on the free surface, the RHS reduces to an integration on just the measurement line,

$$P_s(\mathbf{r},\mathbf{r}_s,\omega)=\int_{m.l.}[P(\mathbf{r}',\mathbf{r}_s,\omega)\nabla' G_0(\mathbf{r}',\mathbf{r},\omega)-G_0(\mathbf{r}',\mathbf{r},\omega)\nabla' P(\mathbf{r}',\mathbf{r}_s,\omega)]\cdot d\mathbf{l}'. \quad (2)$$

This is the formula of P_s wave predicted at $\mathbf{r}$. It removes P_0 wave. When the cable is horizontal, the gradient operator becomes simply the derivative with respect to depth, and d$\mathbf{l}$' becomes the sampling interval dx'

$$P_s(\mathbf{r},\mathbf{r}_s,\omega)=\int_{m.l.}[P(\mathbf{r}',\mathbf{r}_s,\omega)\tfrac{d}{dz'}G_0(\mathbf{r}',\mathbf{r},\omega)-G_0(\mathbf{r}',\mathbf{r},\omega)\tfrac{d}{dz'}P(\mathbf{r}',\mathbf{r}_s,\omega)]dx' \quad (3)$$

When the cable has some regular lateral variation in depth $z'(x')$, where z' is the depth function of offset x', we can derive its normal vector $\mathbf{n}=(-\frac{\frac{dz'(x')}{dx'}}{\sqrt{1+(\frac{dz'(x')}{dx'})^2}},\frac{1}{\sqrt{1+(\frac{dz'(x')}{dx'})^2}})$. So formula (2) becomes

$$\begin{aligned}P_s(\mathbf{r},\mathbf{r}_s,\omega)&=\int_{m.l.}[P(\mathbf{r}',\mathbf{r}_s,\omega)(-\frac{\frac{dz'(x')}{dx'}}{\sqrt{1+(\frac{dz'(x')}{dx'})^2}}\frac{\partial}{\partial x'}+\frac{1}{\sqrt{1+(\frac{dz'(x')}{dx'})^2}}\frac{\partial}{\partial z'})\\&G_0(\mathbf{r}',\mathbf{r},\omega)-G_0(\mathbf{r}',\mathbf{r},\omega)\tfrac{\partial}{\partial n'}P(\mathbf{r}',\mathbf{r}_s,\omega)]dx'\sqrt{1+(\frac{dz'(x')}{dx'})^2} \quad (4)\end{aligned}$$

where $\frac{\partial}{\partial n'}P(\mathbf{r}',\mathbf{r}_s,\omega)$ is the normal derivative of $P(\mathbf{r}',\mathbf{r}_s,\omega)$ with respect to the cable. We will compare formula (3) and formula (4) in numerical examples.

NUMERICAL EXAMPLES

Velocity model is shown in Figure 3. The velocities of water and earth are 1500m/s and 2250m/s, respectively. The water bottom and the air-water boundary are both horizontal. Two different cables will be used to illustrate the effectiveness of formula (4). 2D synthetic data are generated on the cable using the Cagniard-de Hoop method. The advantage of Cagniard-de Hoop method is that it can generate separately any event of P_0 wave and P_s wave. $\frac{\partial}{\partial n'}P(\mathbf{r}',\mathbf{r}_s,\omega)$ is estimated using finite difference with data generated on a secondary cable close to the original cable.

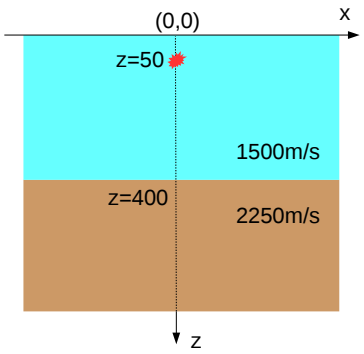

Figure 3: Velocity model and source position. The source is at $(0,50)$. The water bottom is at 400m.

Parabolic Cable

The depth function of the cable is $z=0.0004x^2+100$. The offset is from -400m to 400m. Figure 4a shows the synthetic data along the cable. The top 2 events, which are P_0 waves, are

direct wave and its ghost, respectively. The 4 events beneath, which are P_s waves, are respectively the primary reflected from the water bottom, the source ghost of the primary, the receiver ghost of the primary and the source-receiver ghost of the primary. Figure 4b shows the synthetic P_s wave at depth 95m, which is for comparison with separation result at 95m using Figure 4a. We can use Figure 4b to assess separation results.

Figure 4c is the separated P_s wave at 95m, assuming the cable is flat, i.e. using formula (3). Figure 4d shows the difference between Figure 4c and Figure 4b, using the same color scale as Figure 4c. We can see the difference is very small at near offset but very obvious at far offset, especially for P_0 wave. This is probably because the cable at near offset has small depth gradient and hence the flat cable assumption is valid. Figure 4e and 4f show respectively the separated P_s wave at 95m using formula (4) and its difference with Figure 4b using the same scale. We can see the difference is neglectable, and the strong P_0 wave is fully removed.

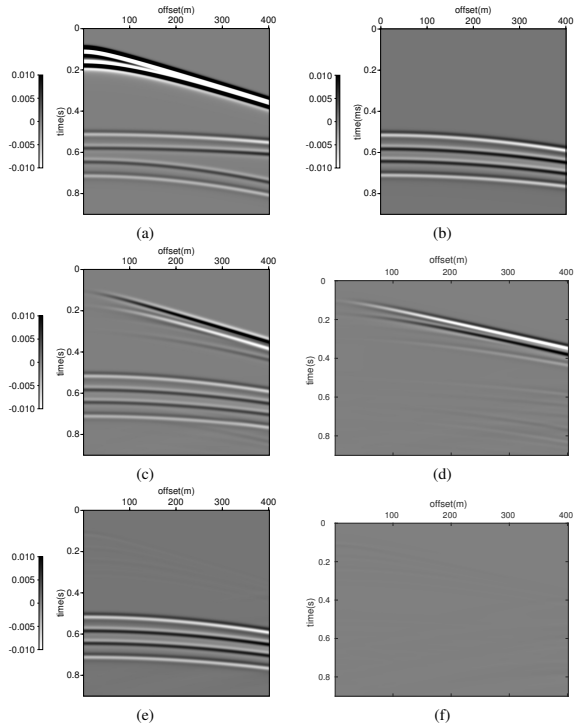

Figure 4: Wave separation results. (a)generated total wavefield by Cagniard-de Hoop method at cable $z = 0.0004x^2 + 100$, (b)generated P_s wave by Cagniard-de Hoop method at $z = 95m$ for comparison, (c)separated P_s wave at $z = 95m$ using formula (3), (d)difference between (c) and (b), (e)separated P_s wave at $z = 95m$ using formula (4), and (f)difference between (e) and (b)

Periodically Semicircular Cable

The above subsection tests formula (4) using a mildly depth-variable cable. The result is good. This subsection tests it using a undulating cable, as shown by Figure 5. The solid line is the primary cable with radius 50m. For normal derivative estimation, a shallower cable is also designed with radius 50.1m or 49.9m, as shown by the dash line.

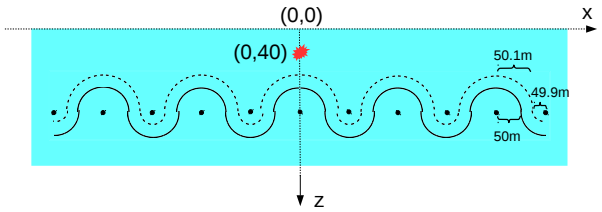

Figure 5: Configuration of the periodically semicircular cable.

Regular spatial sampling interval

Notice that some parts of the cable can be as steep as 90 degree. To avoid as much as possible the deviation of the cable shape in computer implementation, the spatial sampling interval is choosen to be 0.1m. In actual situation, such fine sampling can be achieved by interpolation. Figure 6 compares separation results using formula (3) and using formula (4). As shown by Figure 6c and 6d, because of the cable varies greatly in depth with offset, formula (3) fails to remove P_0 wave and hence the separation result is not satisfactory. Some crossing artifacts appear where there should be no energy events. In contrast, as shown by Figure 6e and 6f, the separation result is much better using formula (4), and only small residues of the direct wave and its ghost remain.

Irregular spatial sampling interval

To further remove the residues of P_0 wave in Figure 6f, smaller spatial sampling interval 0.01m is adopted from offset 45m to 55m, 95m to 105m and so on, where the cable is very steep (shown by Figure 7). Other parts of cables still adopt 0.1m sampling interval. Figure 8 shows the separation result. We can see, the residues of P_0 wave are removed as expected. This is because such fine spatial sampling provides more accurate dl' for the integration.

In the presence of free surface multiple

Finally, we test formula (4) using periodically semicircular cable in the presence of free surface multiples, which are very common in offshore data. For the model shown by Figure 3, the Cagniard-de Hoop method can easily generate free surface multiples of any order. Here we just consider the first order, as shown by Figure 9a, since the energy of higher order multiples is neglectable. The top 2 events represent P_0 wave including the direct wave and its ghost. The next 4 events are respectively the primary reflected from the water bottom, its source ghost, its receiver ghost and its source-receiver ghost. The 4 events at the bottom are the first order free surface multiples of the primary and its ghosts. Figure 9c and 9d show the separation result. As we can see, P_0 waves are removed very well, while P_s waves remain basically intact.

CONCLUSIONS

The 2D acoustic Green's theorem P_0/P_s separation algorithm is developed and tested for depth-variable cables. This is very meaningful for ocean bottom preprocessing when the ocean bottom is not flat, and for on-shore preprocessing since the

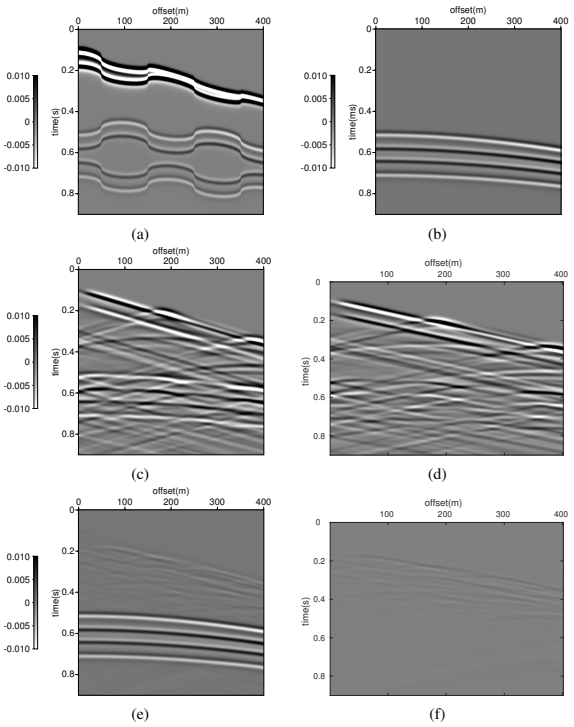

Figure 6: Wave separation results. (a)generated total wavefield by Cagniard-de Hoop method at the primary cable, (b)generated P_s wave by Cagniard-de Hoop method at $z = 95m$ for comparison, (c)separated P_s wave at $z = 95m$ using formula (3), (d)difference between (c) and (b), (e)separated P_s wave at $z = 95m$ using formula (4), and (f)difference between (e) and (b)

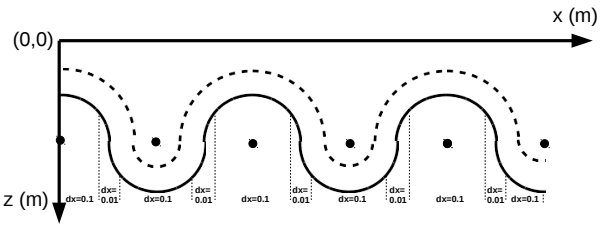

Figure 7: Irregular sampling configuration.

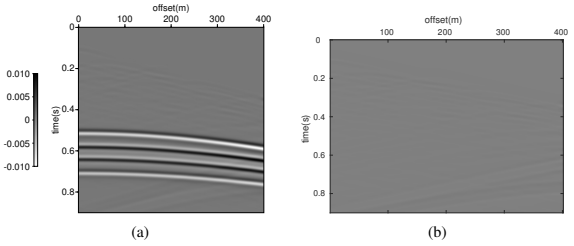

Figure 8: Wave separation results. (a)separated P_s wave at $z = 95m$ using formula (3), and (b)difference between (a) and Figure 6b

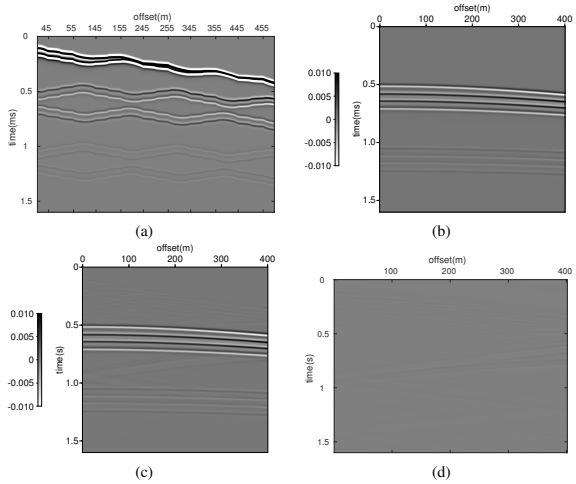

Figure 9: Wave separation results. (a)generated total wavefield by Cagniard-de Hoop method at the primary cable (b)generated P_s wave by Cagniard-de Hoop method at $z = 95m$ for comparison, (c)separated P_s wave at $z = 95m$ using formula (3), and (d)difference between (c) and (b)

earth's surface is usually laterally variant. Numerical examples have shown that if data are acquired by nonhorizontal cables, the constant depth assumption is still valid when the cable is just slightly curved. The depth-variable cable version of Green's theorem derived in this paper avoids such limitation, by incorporating the cable's real depth function of offset. As results show, if the cable is not horizontal, spatial sampling interval is the main factor that determines whether the separation result is satisfactory. Since the depth-variable cable version of Green's theorem takes the cable's exact shape function into consideration, we can get good deghosting result even if the cable is steep. The last numerical case demonstrates that when free surface multiples exist, the free surface multiples are not compromised in separation since they belong to P_s wave. This is encouraging for wavelet estimation and further processing including multiple attenuation. This would allow the benefit, from Green's theorem wavefield separation, for towed streamer data to be extended and utilized for on-shore and ocean bottom acquisition, where the measurement can at times be far from horizontal.

ACKNOWLEDGEMENTS

We thank the M-OSRP sponsors for their encouragement and support. We would like to thank Jingfeng Zhang of BP for his great work in his PhD dissertation and his fundamental implementation of Cagniard-de Hoop method. We would like to thank all M-OSRP members. Their comments and suggestions are worthwhile and have benefited this paper.

REFERENCES

Guo, Z., A. B. Weglein, and T. H. Tan, 2005, Using pressure data on the cable to estimate the seismic wavelet: 75th Annual International Meeting, SEG, Expanded Abstracts, 2390–2393.

Keho, T., A. B. Weglein, and P. G. Rigsby, 1990, Marine source wavelet and radiation pattern estimation: 75th Annual International Meeting, SEG, Expanded Abstracts, 1655–1657.

Mayhan, J., 2013, Wave-theoretic preprocessing to allow the inverse scattering series methods for multiple removal and depth imaging to realize their potential and impact: methods, examples, and added value: Ph.D. dissertation, University of Houston.

Mayhan, J. D., and A. B. Weglein, 2013, First application of Green's theorem-derived source and receiver deghosting on deep-water gulf of mexico synthetic (seam) and field data: Geophysics, **78**, WA77–WA89.

Morse, P. M., and H. Feshbach, 1953, Methods of theoretical physics: International Series in Pure and Applied Physics, New York: McGraw-Hill, 1953, **1**.

Tang, L., 2014, Developing and analyzing Green's theorem methods to satisfy prerequisites of inverse scattering series multiple attenuation for different types of marine acquisition and extending prerequisite satisfaction to on-shore exploration: Ph.D. dissertation, University of Houston.

Weglein, A. B., F. V. Araújo, P. M. Carvalho, R. H. Stolt, K. H. Matson, R. T. Coates, D. Corrigan, D. J. Foster, S. A. Shaw, and H. Zhang, 2003, Inverse scattering series and seismic exploration: Inverse problems, **19**, R27–R83.

Weglein, A. B., J. D. Mayhan, L. Amundsen, H. Liang, J. Wu, L. Tang, Y. Luo, and Q. Fu, 2013, Green's theorem deghosting algorithms in (k,omega) (eg, p-vz deghosting) as a special case of (x,omega) algorithms (based on Green's theorem) with: (1) significant practical advantages and disadvantages of algorithms in each domain, and (2) a new message, implication and opportunity for marine towed streamer, ocean bottom and on-shore acquisition and applications: Journal of Seismic Exploration, **22**, 389–412.

Weglein, A. B., and B. G. Secrest, 1988, Wavelet estimation for a multidimensional acoustic or elastic earth: 58th Annual International Meeting, SEG, Expanded Abstracts, 936–938.

Weglein, A. B. and B. G. Secrest, 1990, Wavelet estimation for a multidimensional acoustic or elastic earth: Geophysics, **55**, 902–913.

Weglein, A. B., T. H. Tan, S. A. Shaw, K. H. Matson, and D. J. Foster, 2000, Prediction of the wavefield anywhere above an ordinary towed streamer: Application to source waveform estimation, demultiple, deghosting, data reconstruction and imaging: 70th Annual International Meeting, SEG, Expanded Abstracts, 2413–2415.

Zhang, J., 2007, Wave theory based data preparation for inverse scattering multiple removal, depth imaging and parameter estimation: Analysis and numerical tests of Green's theorem deghosting theory: Ph.D. dissertation, University of Houston.